Article

Not peer-reviewed version

Advanced Performance Photoluminescent Organic Light-Emitting Diodes Enabled by a Natural Dye Emitters Considering a Circular Economy Strategy

Vasyl G Kravets *, Vasyl Petruk, Serhii Kvaterniuk, Roman Petruk

Posted Date: 26 November 2025

doi: 10.20944/preprints202511.2081.v1

Keywords: organic light-emitting diodes; natural dyes; MoS2 monolayer; natural dye –MoS2 light emitter; photoluminescence spectroscopy

 doi:10.20944/preprints202511.2081.v1

Article

Advanced Performance Photoluminescent Organic Light-Emitting Diodes Enabled by a Natural Dye Emitters Considering a Circular Economy Strategy

Vasyl G. Kravets [1,*], Vasyl Petruk [2], Serhii Kvaterniuk [2] and Roman Petruk [2]

[1] Department of Physics and Astronomy, the University of Manchester, Manchester, UK

[2] Department of Ecology, Chemistry and Environmental Protection Technologies, Vinnytsia National Technical University, Vinnytsia, Ukraine

* Correspondence: vasyl.kravets@manchester.ac.uk

Abstract

Organic optoelectronic devices receive appreciable attention due to their low cost, ecology, mechanical flexibility, band-gap engineering, lightness, and solution process ability over a broad area. Here, we designed and studied an organic light-emitting diodes (OLEDs) consisting of assembly of natural dyes extracted from of noble fir leaves (*evergreen*) and blue hydrangea flowers and mixed with poly-methyl methacrylate (PMMA) as a light emitters. We experimentally demonstrate effective red and green photoluminescence due to the excitation natural dye-PMMA nanostructures by laser/photodiode blue light. The UV-Visible absorption and photoluminescence spectroscopy, ellipsomentric and Fourier transforms infrared methods together with optical microscopy were achieved for confirming and characterizing the properties of light-emitting diodes based on natural dyes. We highlighted the optical and physical properties of two different natural dyes, and demonstrated how such characteristics can be exploited to make efficient LED devices. A strong pure red emission with narrow full-width at half maxima (FWHM) of 23 nm in the noble fir dye-PMMA layer and a green emission with FWHM of 45 nm in blue hydrangea dye-PMMA layer have been observed. It was revealed that adding the MoS_2 monolayer to the nanostructure can significantly enhance the photoluminescence of natural dye due to strong correlation between emission bands of the inorganic-organic emitters and back mirror reflection of the excitation blue light from monolayer. Based on investigation of two natural dyes we demonstrated viable pathways for scalable manufacturing of the efficient OLEDs consisting of assembly of natural dyes -polymer through low-cost, pure ecological and human convenient processes.

Keywords: organic light-emitting diodes; natural dyes; MoS_2 monolayer; natural dye –MoS_2 light emitter; photoluminescence spectroscopy

1. Introduction

Organic light-emitting diodes (OLEDs) are at the forefront of modern display and lighting technologies, powering nearly everything from smartphone screens to large monitors. A key advantage of organic photoluminescent (PL) materials lies in their outstanding flexibility of chemical modification, high contrast, wide color gamut, fast response, lightweight, recising control over their fluorescence behaviours for the development of customized materials for specific applications. [1,2]. Despite their recent achievement in consumer electronics, there are still some deficiencies in OLED technology that limit further improvement of emission performance. Note that their rapid growth in consumer electronics, from smartphone displays to large monitors, is exacerbating the problem of end-of-life sustainability. Traditional electronic devices often have complex, multi-layered constructions where components are bonded together using irreversible methods, such as strong adhesives, making it extremely difficult to extract valuable materials. Moreover, adding functional

 doi:10.20944/preprints202511.2081.v1

groups to change PL colors still suffer intricate molecular designs and multi-step synthesis processes. [2,3]. These challenges require new strategies that enabling efficient and scalable methods to altering their PL properties. One of the most viable solutions for realising the development of new organic light-emitting diodes is involving the incorporation of natural materials for the fabrication of high effective devices [4]. Natural dyes are earth abundant, easily extractable, safe material causes no environment threat. They can be extracted from flowers petals, leaves, roots and barks in the form of anthocyanin, carotenoid, flavonoid and chlorophyll pigments. In natural dyes chlorophylls are photoactive molecular building blocks existent in the most photosynthetic systems. Usually, dyes molecules capture UV-Vis-IR light to make photosynthesis and can converts it into photoluminescent emission of different colors [5]. Natural dye molecules turn over billions of times and remain stable for years. Chlorophylls in the natural dyes are biomolecules that are both environmentally sustainable and harmless, as well as the primary component of plant species that use light energy for photosynthesis and perform better in the near ultraviolet making them a preferred light-emitting material for OLEDs. [6–8]. It will be important to borrow from nature the same physics-chemical principles to fabricate new OLEDs. The natural dyes are luminescent material satisfying a set of requirements to make it suitable: their PL spectrum can cover a wide range of the visible band to allow for rendering all colors visible to the human eye. It is well known that developing organic luminophores with strong and narrowband emission capabilities is thus crucial for the further advancement of OLEDs, which yet is much more challenging. For example in OLED displays, each subpixel should emit a distinct spectrum for red, green, and blue, with each color appearing as a relatively narrow peak in a spectrum range to ensure high color purity and clear separation of primary colors. The demands of eco-friendly technologies to produce a high quality of OLEDs a large scale remains also a big challenge.

Here, we suggest using natural dyes as an environmentally and economically superior alternative to traditional synthetic dyes for developing OLEDs, which often require a complex synthesis and can be toxic. We have shown that the process of synthesis photoluminescent cells based on natural dyes is a low-costly which can be considered as a viable option for OLEDs in future application research. To facilitate the extraction of natural dye compounds, a solvent-assisted extraction method utilising methanol was employed. Methanol is widely recognized as an effective and eco-friendly solvent for natural dye extraction due to its high polarity, ability to dissolve abroad range of organic compounds, and preservation of dye stability. In this work, the broad spectra of optical properties of fabricated natural dye-PMMA nanostructures have been studied in UV-Vis-IR spectral range using different experimental methods. We used the photoluminescent features of chlorophyll dyes derived from noble fir leaves (*evergreen*) and blue hydrangea flowers and mixed ones with poly-methyl methacrylate (PMMA) to create the OLEDs with two distinct fluorescence colors of green and red with narrow full-width at half maxima (FWHM). It was shown that such natural dye- polymer composites can be conveniently manufactured as color conversion layers for application in light–emitting devices to meet high performance. Obtained experimental results show that fluorescent natural-dye-PMMA layers can be combined with standard inorganic GaN blue light photodiode (PD) to create a electroluminescent OLEDs with three distinct colors, such as red, green, and blue (last color is due to mother PD emission). It was revealed that transferring on the substrate MoS_2 monolayer can significantly enhance photoluminescent performance of the natural dye-PMMA layers. Such combination of the ultrathin two dimension semiconductors and natural dyes can be appeared as an efficient means to improve the emission behaviours of organic light-OLEDs due to overlapping the PL bands of mono- and dye layer and extraordinal refractive index of the MoS_2.

In the present investigation, only two natural dyes extracted from noble fir leaves (*evergreen*) and blue hydrangea flowers were deployed as photoluminescent layers for developing of OLEDs to attract attention for novel organic devices with amazing performances and high efficiency. This study demonstrates viable pathways for manufacturing of efficient OLEDs through low-cost and ecologically promising processes.

 doi:10.20944/preprints202511.2081.v1

2. Experimental Results and Discussion

Preparation of Samples

Chlorophyll dye was extracted using the procedures reported by Schiller *et al*., for spinach leaf [9]. Fresh and healthy leaves from the noble fir (or Christmas Tree) and blue hydrangea flowers were collected locally and rinsed thoroughly first with tap water followed by distilled water to remove all the dust and unwanted visible particles, cut into small pieces and dried at room temperature. 10 g of noble fir or blue hydrangea was crushing using mortar into small size and powdered dry leaves were put in different beakers and 100 ml of methanol was added to each beaker. All samples were left in the cupboard for a week. Chlorophyll based samples were filtered twice through Millex HV (0.2 μm) filter membrane and the filtrates stored in the cupboard for analysis and future use. Then prepared chlorophyll dye dispersion was introduced to the Poly(methyl methacrylate) (PMMA 950, 3% anisole) solution under continuous mixing. Chlorophyll dye - PMMA hybrid solution were prepared by mixing corresponding dye-methanol dispersion with 33, 50 and 67 vol. % of PMMA 950, 3% anisole liquid. Resulting mixture was placed into the ultrasonic bath for 30 minutes with the frequency of 37 Hz using Degas mode for preparing homogeneous chlorophyll dye based liquid. The maximal photoluminescence efficiency and stability of final solution was been achieved for compounds of approximately equal volume of chlorophyll dye and PMMA. Due to this fact, we focus below on the properties of 50 % vol. dye-PMMA solutions. As substrate we used the standard Si/SiO_2(90 nm) wafers. Chlorophyll dye-PMMA solution was spin coated on Si/SiO_2 substrate with a small rotating speed ~500 rpm for obtaining thickness of film ~1 μm. Finally the samples were baked at 150 °C on hot plate during 15 min to evaporate residual methanol-anisole liquid and obtain polymerised stable layer.

Noble Fir Blue Hydrangea

a) b)

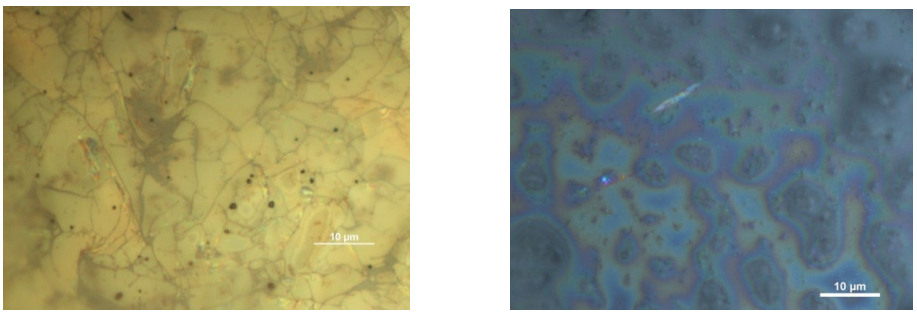

Noble Fir Blue Hydrangea

Figure 1. Preparation of noble fir dye-PMMA and blue hydrangea dye-PMMA nanostructures**.** (a,c) Representative optical microscopy images showing noble fir dye-PMMA and blue hydrangea dye-PMMA cells formed under spinning rates of 500 rpm. Inset: typical leaves of the noble fir and blue hydrangea flowers together with derivatives chlorophyll dye in methanol solution.

 doi:10.20944/preprints202511.2081.v1

3. Characterisation of Samples

3.1. Optical Microscopy Images

By using different types of natural dyes, it is possible to create thin layers that shine in various colors, including blue, green and red. Representative optical microscopy images showing noble fir and blue hydrangea chlorophyll cells entrapped within PMMA matrix (Figure 1). Note that natural dye-PMMA composite form a glowing layers with different colors, which can bright enough emission under illumination from microscopy lamp with broad visible spectrum.

3.2. Photoluminescence Spectroscopy

The photoluminescence (PL) spectra in the range from 400 to 900 nm were analysed using a diffraction spectrometer, Horiba Ltd., Japan. Room temperature PL emission was measured with excitation by GaN-based light emitting diode laser with λ=405 nm and half-width of $\Delta\lambda$~2 nm [10,11]. In the case of proposed OLED-like structure we excited the natural dye-PMMA layers at a wavelength of λ=440 nm and half-width of $\Delta\lambda$~25 nm, which are a typical characteristics of GaN-based LEDs on which a organic luminophor coating could be applied for white light rendering.

3.3. Reflection/Absorption Spectroscopy

Absorbance spectra of natural dyes in PMMA matrix were measured at room temperature using two different methods. First, the absorbance was extracted from experimental data of the diffuse reflectance determined by employing a fiber-coupled spectrometer (USB4000, Ocean Optics) and applying the Kubelka-Munk algorithm [12]. The Kubelka-Munk equation provides a relationship between the diffuse reflectance (R_{dif}) of a film and its absorption (k) and scattering (s) coefficients, typically expressed as the Kubelka-Munk function in the common form, $k/s = (1-R_{dif})^2 / 2R_{dif}$. This method is widely applied in diffuse reflectance spectroscopy to determine optical properties like the band gap of materials by converting measured reflectance into absorption spectra in approximation of s=1 [13].

3.4. Ellipsometric Measurements

To determine the optical absorption of fabricated natural dye - PMMA samples we also use the ellipsometry method. We have measured optical constants $n^*=n+ik$ of the fabricated layers on the Si/SiO_2 substrate by employing a variable angle focussed-beam spectroscopic ellipsometer Woollam M 2000F. This ellipsometer is based on the rotating polariser-compensator-analyser setup and utilises diode array spectrophotometer to extract spectral ellipsometric parameters. The ellipsometer is equipped with the 75 W Xe arc lamp and measures ellipsometric parameters Ψ and Δ in the wavelength range of 240-1200 nm. The spot size on the sample was approximately 50 μm × 70 μm for ~60-70° angles of incidence. Two ellipsometric parameters Ψ (ellipsometric reflection) and Δ (ellipsometric phase) are related to the sample reflection as: $\tan(\Psi)\exp(i\Delta) = r_p/r_s$, where r_p and r_s are the amplitude reflection coefficients for p- and s-polarized light. In addition to ellipsometric parameters Ψ and Δ, the ellipsometer allowed us to separately measure $R_p=|r_p|^2$ and $R_s=|r_s|^2$ providing the intensity reflections for p- and s-polarised light, respectively. The main ellipsometric formula can be written as [14,15]

$$\rho = \frac{r_p}{r_s} = \tan\psi e^{i\Delta} \tag{1}$$

$$n^* = n_2 - ik_2 = \{\sin^2\theta_i + \sin^2\theta_i \tan^2\theta_i \frac{(1-\rho)^2}{(1+\rho)^2}\}^{1/2} \tag{2}$$

 doi:10.20944/preprints202511.2081.v1

Using the standard Woollam's ellipsometric software in the model of bulk combination of assembly natural dye - PMMA structure it is possible find the complex optical constants $n^*=n+ik$ [14–16].

Brewster angle in visible region. For this incident angle the ellipsometric measurement is the most sensitive and precise [15]. From extracted values of the optical constants n, k we can estimate the absorption coefficient, $\alpha=4\pi k/\lambda$ (where λ is the wavelength of the incident light). This absorption coefficient, α is the main characteristic of the Lambert's law: $I=I_0\exp(-\alpha t)$ (where I_0, I is the intensity of the incident and transmitted light, respectively, and t is the thickness of film [17].

3.5. Fourier Transforms Infrared Spectroscopy

Fourier Transform Infra-Red (FTIR) spectroscopy was performed with the help of a Bruker Vertex 80 system and a Hyperion 3000 microscope. A variety of sources and detectors, combined with aluminium coated reflective optics enable this system to be used from visible to mid-IR wavelengths [18].

3.6. Photoluminescence Spectra

Room-temperature photoluminescence spectra of chlorophyll dye of noble fir and blue hydrangea show a non-symmetric dependences with peaks at λ~675 nm (red light) and λ~560 nm (green light), respectively (Figure 2a,b). Under laser 405 nm excitation the 675 nm emissions emerges as the main component for noble fir dye-PMMA layer and the occurrence a small peak at 722 nm which indicates the existence of two luminescence species. In contrast to noble fir-PMMA layer, the PL spectra of blue hydrangea dye-PMMA contain an additional shoulder near λ~525 nm, at shorter wavelength than a strong main peak at λ~560 nm. The spectral position of PL peaks of noble fir dye-PMMA and blue hydrangea dye-PMMA do not change with a measurement in the different areas of samples. Colour purity is another key criterion of OLEDs, which depends on the width of the emission spectrum and is typically measured by the full-width at half-maximum (FWHM). It should also be noted that the PL peak in the red region λ~675 nm demonstrates smaller FWHM $\Delta\lambda$~23 nm than ones in the case of the short-wavelength (λ~560 nm) of green PL emission ($\Delta\lambda$~45 nm) (Figures 2a,b). We measured the efficient yield of the PL noble fir dye which usually refers to the intensity of emitted photons over the intensity of excitation laser light. For determining of the efficiency PL the ratio between of intensity PL at λ~675 nm and the corresponding value of the peak of exciting laser emission (λ~405 nm) was evaluated: $\eta=I_{PL(max)}/I_{laser(max)}\approx0.17$ (Figure 2c).

The intensity of PL of chlorophyll dye in the red region can be significantly enhanced by adding into device the MoS_2 monolayer between substrate Si/SiO_2 and natural dye-PMMA nanostructure. Figure 2d demonstrates the boosting of PL emission intensity more than 5 times due to presence of MoS_2 monolayer in fabricated device. Note that the MoS_2 is effective luminescent materials with peak of emission near the 675 nm in the same region as for noble fir dye (compare Figures 2a,c and e). Moreover, a small FWHM of PL for MoS_2 monolayer can significantly enhance the efficiency of top-emitting natural dye-PMMA nanostructure due to significant overlapping between the both PL spectra. Note that MoS_2 monolayer possesses also the high reflectance in the visible range of spectra due to the large values of the real part of the refractive index (Figure 2f). Optical constants of MoS_2 monolayer (with thickness about 0.7 nm) were calculated using the three-phase ellipsometric model consisting of the substrate Si/SiO_2(90nm), MoS_2 monolayer and ambient (air) based on measured ellipsometric parameters Ψ and Δ for different incidence angles (50-70 degs.). Two dominant peaks are observed at the wavelength of ~660 nm and ~607 nm in the k and R plots, which are related to A, B excitonic peaks. In the shorter wavelength range 370-470 nm occurred C, D excitonic peaks [19]. Note that monolayers MoS_2 display extraordinary large value of the real part of the refractive index about n~5-6 at λ~400-500 nm, Figure 2f. Such highly reflective MoS_2 monolayer works as back reflection mirror and promote to collect the more part of excited light from blue laser (or photo-diode) in chlorophyll dye-PMMA nanostructure. The PL efficiency of the $Si/SiO_2/MoS_2$/noble fir dye–PMMA nanostructure is closed to the PL quantum yield (PLQY) of commonly used reference material such

 doi:10.20944/preprints202511.2081.v1

as rhodamine R6G in an ethanol solution (PLQY of 94%) [20]. Usually, the PLQY is a measure of a PL's efficiency, defined as the ratio of the number of photons emitted by fluorescence to the number of photons absorbed.

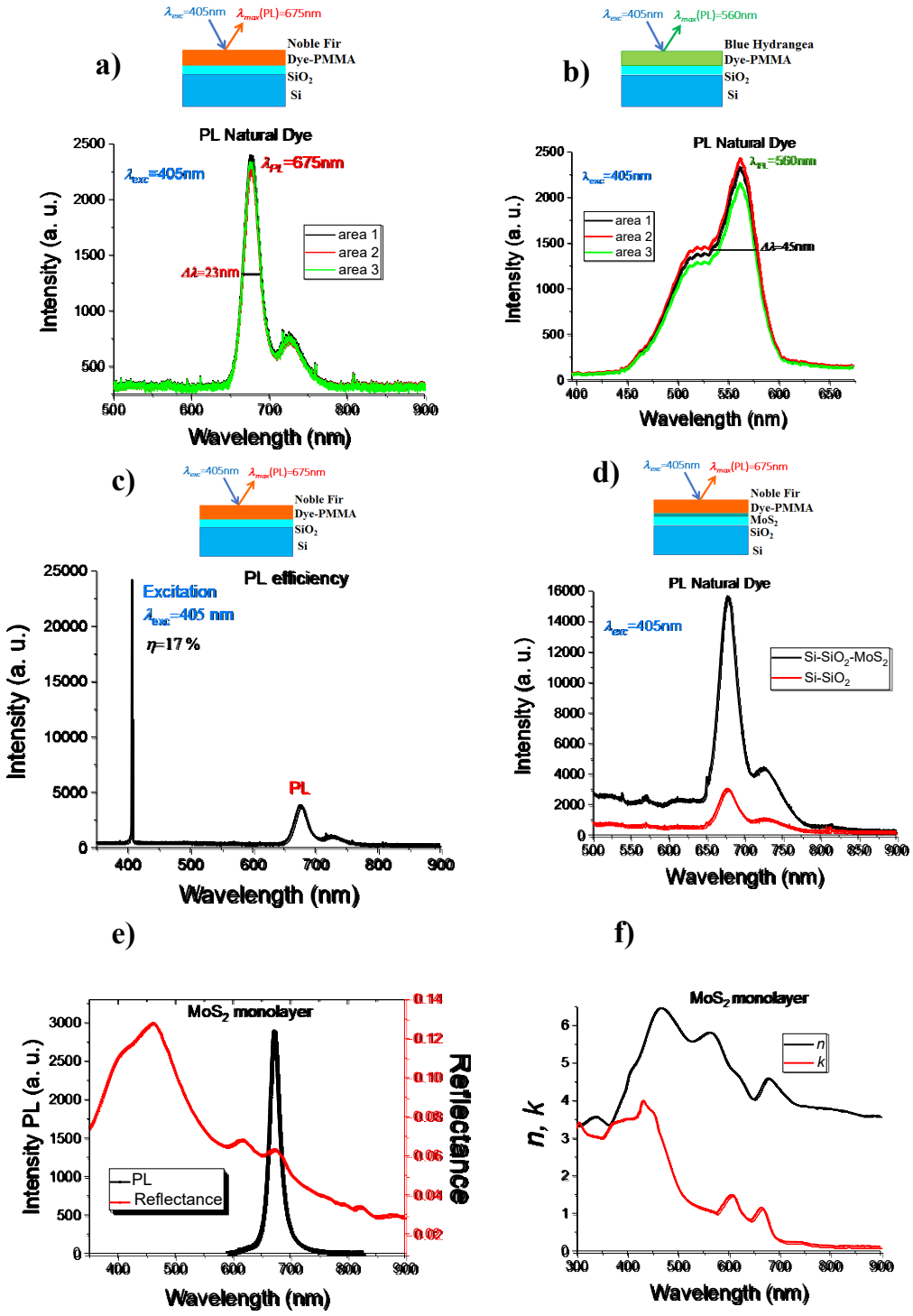

Figure 2. Photoluminescence spectra excited by GaN laser at a wavelength of 405 nm: (a,b) for noble fir dye-PMMA and blue hydrangea dye-PMMA nanostructures, respectively. (c) Estimation of the PL efficiency based on ratio of PL intensity to laser excitation intensity for noble fir dye-PMMA layer. (d) Enhancement of PL efficiency due to overlapping of PLs from noble fir dye-PMMA and MoS_2 monolayer. Inset: schematics of the measurement nanostructure. (e, f) Optical characteristics of the MoS_2 monolayer: (e) Strong reflectance and photoluminescence of MoS_2 monolayer; (f) the complex refractive index of MoS_2 monolayer.

 doi:10.20944/preprints202511.2081.v1

3.7. Absorption Spectra

The optical properties of noble fir dye-PMMA and blue hydrangea dye-PMMA nanostructures were evaluated from diffuse reflection by applying the Kubelka-Munk approach and ellipsometric measurements. The UV–Vis – near IR absorption spectra of chlorophyll dyes in PMMA matrix is shown in Figures 3a. The two types of chlorophyll dyes exhibit absorption bands at wavelengths of 400 and 670 nm. Moreover, the absorption peak of the blue hydrangea dye-PMMA nanostructure is severely blue-shifted by ~40 nm from 400 nm compare to spectral position for the noble fir dye-PMMA ones. It is well known that these major types of absorption bands originate from chlorophyll '*a*' and chlorophyll '*b*' [21,22]. Note that the blue hydrangea dye-PMMA nanostructure displays additional band at λ~442 nm (Figure 3a). Chlorophyll *b* produces main absorption peak at a short wavelength absorption (400-500 nm). Chlorophyll *a* can be considered the primary photosynthetic pigment and has an in vivo long-wavelength absorption maximum ~680 nm, which shifts to ~670 nm in organic solvents. Chlorophyll *c* has its maximum absorption λ~450 nm what we observed for the blue hydrangea dye-PMMA. For total picture we can mention that chlorophyll *d* absorbs in vivo at 720 nm or in the far-red region [22].

Microscopy origin of absorption in natural dye can be associated with corresponding π–π^* transition which originates from the aromatic molecular structure of the dyes >C=O group and mainly boosts at wavelengths near 400 nm. On the other hand, the blue hydrangea dye-PMMA nanostructure manifests the band beyond 500 nm, which arises due to the transfer of electrons between the donor and acceptor molecules, through the π-bridge upon light absorption (through the non-bonding orbitals, *n*). The absorption moves to longer wavelength ~700-730 nm as the amount of delocalisation in the dye molecules increases [23]. Thus the both noble fir dye-PMMA and blue hydrangea dye-PMMA nanostructures show up three intense peaks in the range of 300–700 nm; for both dye the first sharp peak represents the presence of aromatic structure (300–420 nm), second absorbance peak represents the presence of n–π^* transition in >C=O group (430-500 nm), and third represents the conjunction (delocalization of electronic state in the dye molecules) of the compound (670-720 nm).

The resulting complex refractive index $n^*=n+ik$ is extracted from ellipsometric measurements and plotted for noble fir dye-PMMA and blue hydrangea dye-PMMA nanostructures in Figure 3b, showing a correlation between dependences for absorbance *A* and the imaginary parts, *k* presented in Figures 3a, b, respectively. The spectra of the imaginary parts, *k* exhibits two main bands at λ~400 and 670 nm. We observed the increase of the amplitude *k* for blue hydrangea dye-PMMA nanostructure together with a shift to high photon energy of the absorption peak near 400 nm. The most obvious tendency for the real parts of the refractive index, *n* is a general oncoming to the values typical for pure PMMA matrix and their modulation in the blue range of the spectra by adding of natural dye. Note that features in the *n* and *k* spectra (Figure 3b) look not such bright as in the dependences presented in Figure 3a for absorption because the ellipsometric measurements contain large part of the diffuse scattering which is very difficult to include in the approach for evaluation real *n* and *k* (it will be correct to tell about effective values of *n* and *k*).

It is well known that an ideal luminescent material should exhibit a large Stokes shift to minimize the spectral overlapping of the tails of the absorption and emission spectra, ensuring that the reemitted photons do not get reabsorbed by the neighbouring dyes [24]. Our measurement of PL emission by chlorophyll dyes demonstrated a large Stokes shift between excitation laser light of 405 nm and PL peaks which is located at 560 nm for blue hydrangea dye-PMMA and 675 nm for noble fir dye-PMMA nanostructures, respectively.

 doi:10.20944/preprints202511.2081.v1

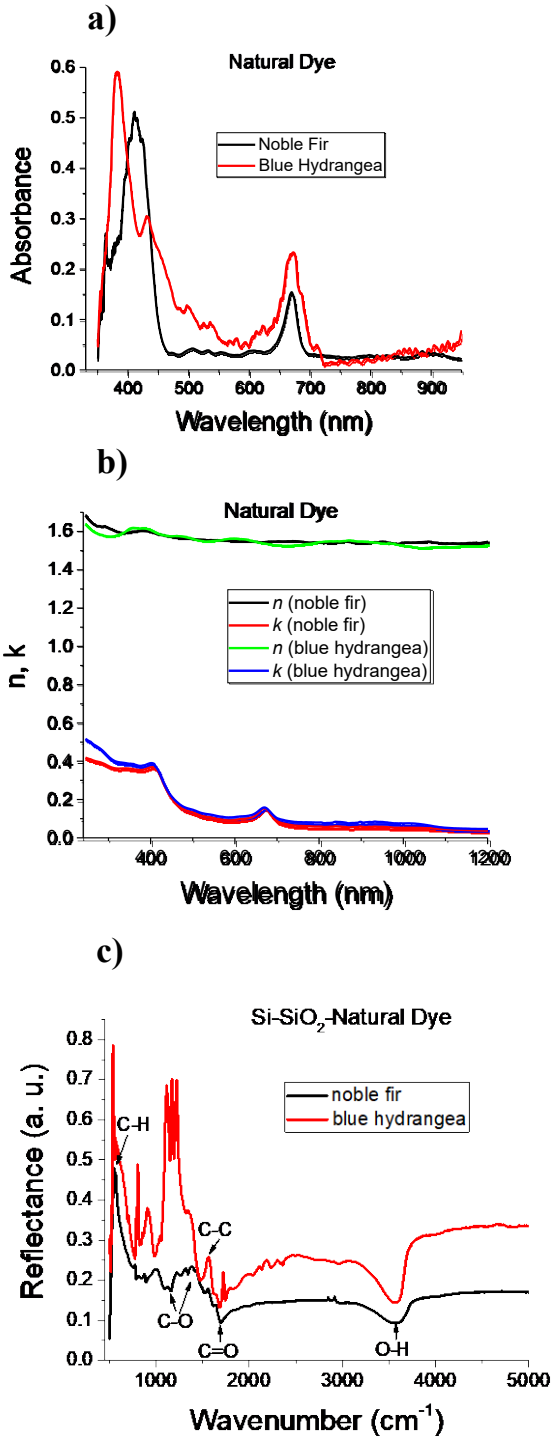

Figure 3. The UV-Visible-near IR absorption spectra. (a) Absorption coefficients for noble fir dye-PMMA and blue hydrangea dye-PMMA nanostructures derived from the diffuse reflectance using Kubelka–Munk approach. (b) The complex refractive index $n^*=n+ik$ extracted from ellipsometric measurements for noble fir dye-PMMA and blue hydrangea dye-PMMA nanostructures. (c) Fourier transforms infrared (FTIR) spectra for noble fir and blue hydrangea dyes deposited on Si-SiO_2 substrate.

3.8. FTIR Spectroscopy

The FTIR spectra offered significant information about the dyes' chemical structures. In the O–H stretching area, a peak was detected at 3560 cm^{-1} for pure noble fir dye deposited on Si-SiO_2 substrates (we excluded the contribution in FTIR spectra from PMMA molecules, and reflectance was measured respect to Ag mirror), and this peak moved to 3580 cm^{-1} for blue hydrangea dye (Figure

 doi:10.20944/preprints202511.2081.v1

3c). This specific site is suggestive of hydroxyl (O–H) group stretching vibrations, which are normally linked with the presence of phenols in chlorophyll dye *b* [23]. Furthermore, the region between 1650 and 1750 cm^{-1} exhibited C═O bond-specific peaks. Similarly, the peak at 1470 cm^{-1} indicated the occurrence of C–C stretching, a characteristic feature of aromatic compounds. The both FTIR spectra show clear peaks at about 1100 and 1300 cm^{-1}, but the region between those peaks varies strongly between these spectra. Note that C–O stretching vibrations in chlorophyll *b* usually are connected with a spectral region of 1000–1300 cm^{-1}. Thus, various vibrational modes were identified in the chlorophyll dye's FTIR spectra. The broad peak around 3570 cm^{-1} shows OH group stretching, the peaks around 1690 cm^{-1} indicates C═O. Similarly, C═C stretching showed at 1675 cm^{-1}, and C–O vibrations showed at 1143 cm^{-1}. Furthermore, the appearance of the bandwidth at 600 cm^{-1} proved the occurrence of the C–H bond bending in aromatic rings (Figure 3c) [23].

3.9. PL Performance Based on Natural Dyes Excited by Blue GaN Photodiode

Developing high-performance blue, green and red OLEDs is a major challenge, and emitters are critical for overcoming this issue. To evaluate the PL performance of natural dye nanostructures, we covered blue gallium nitride (GaN) light-emitting photodiodes (PD) by a corresponding dyes-PMMA nanostructure as shows in the inset of Figure 4. Such PD is essential for next-generation display technologies owing to their high resolution, low power consumption, and long lifespan. Spectral stability of the PD emission was evaluated across a driving voltage range of 2.5–4.0 V and current ~1 mA. It was found that the GaN PD exhibits a small redshift (439-443 nm) as the voltage elevated, whereas the PD maintains a narrow emission wavelengths ($\Delta\lambda$~20 nm) and uniform intensity distribution throughout the same voltage range. Thus the bottom-emitting blue PD emit at λ~440 nm which excites the PL in the top noble fir dye-PMMA or blue hydrangea dye-PMMA nanostructures (Figures 4a,b). The optical transmittance reaches approximately 80% at both the emission wavelengths of the green and red natural dye-PMMA nanostructures (560 and 675 nm), indicating minimal optical loss as photons pass through the OLEDs. Top-emitting chlorophyll dyes devices achieve enhanced red and green colors purity (FWHM of 25-45 nm) under a low running voltage applied to GaN PD (2.5-3.5 V and currents of 0.5 mA) which provides brightness of ~900 cd m^{-2}. This study provides an important strategy to develop high-performance green and red OLEDs based on natural dyes. Furthermore, need to stress that our experimental results demonstrates that photoluminescent natural-dye-PMMA nanostructures can be combined with standard inorganic GaN blue light PD to create electroluminescent OLEDs with three distinct colors, such as red, green, and blue (where, last color is directly associated with PD emission).

 doi:10.20944/preprints202511.2081.v1

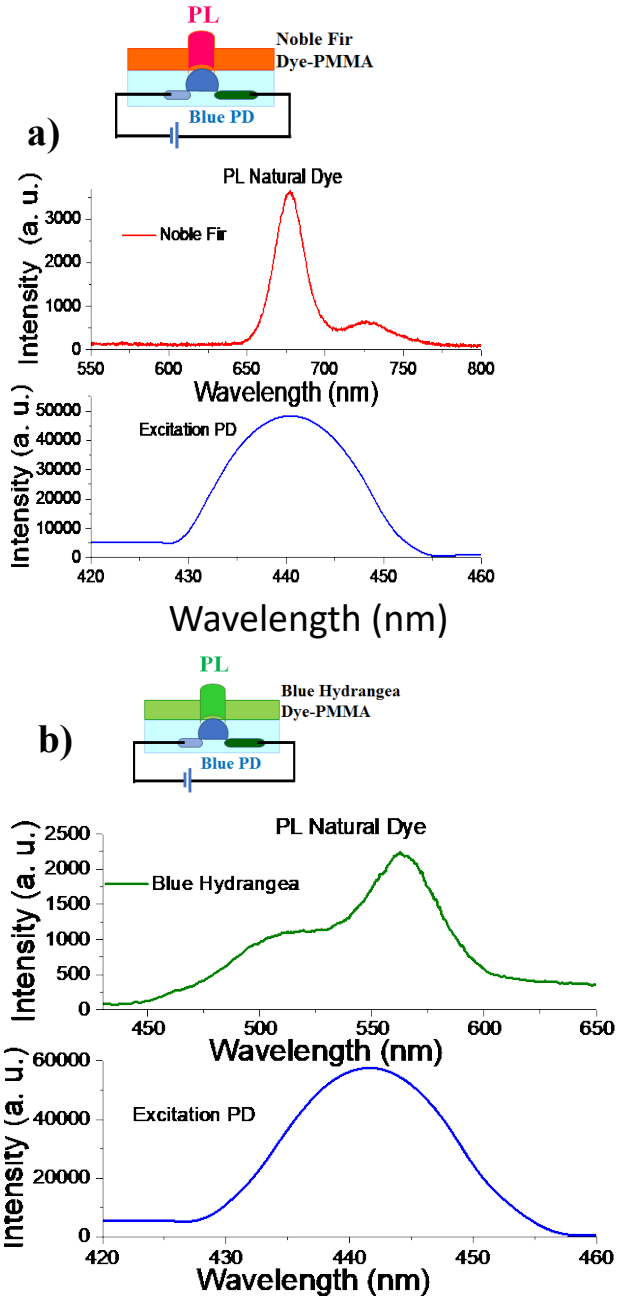

Figure 4. Analogical OLEDs based on natural dyes. (a,b) Bottom-emitting blue GaN PD emit at λ~440 nm cause the PL in the top noble fir dye-PMMA (a) and blue hydrangea dye-PMMA (b) nanostructures. Inset: schematics of the fabricated devices based on natural dyes.

3.10. A Circular Economy Strategy for Photoluminescent Organic LEDs Based on Natural Dyes

In this study we show that a carefully designed combining nature dye thin film with TMDs monolayer it is possiible to turn a single blue emitter into a tunable different color's OLED using low cost materials already familiar to manufacturers. Suggested design of OLED could significantly reduce the ecological footprint and cost of OLED manufacturing, as it requires fewer scarce inputs and fewer processing steps. These OLEDs can work well on flexible surfaces, opening options for sleek luminaires, thin backlights, and future smart-building panels. The next step for the researchers should be to explore brightness, efficiency, and long-term stability in order to advance lab prototypes into real-world lighting products. It importantly is to analyse the creation of OLEDs based on natural dyes to ensure the full circularity of this environmentally friendly prototype. Natural dyes, particularly chlorophylls, promise an environmental advantage of proposed technology. They are

 doi:10.20944/preprints202511.2081.v1

bioavailable, non-toxic, low-cost and have a large Stokes shift (e.g., excitation at 405 nm, emission at 675 nm), which prevents reabsorption and increases device efficiency. The integration of the PMMA polymer matrix and the functional MoS_2 monolayer promote to create a "circular paradox" - when increasing in technical efficiency leads to a decrease in recycling efficiency. Note that PMMA is a thermoplastic that is ideal for chemical recycling (depolymerisation) back to the pure monomer methyl methacrylate (MMA). This recycling significantly reduces the carbon footprint compared to the production of fossil-fuel-based virgin plastic. On the other hand monolayer MoS_2 is an extremely valuable two-dimensional semiconductor, essential for enhancing photoluminescence in devices. Usually, its integration is typically done via polymer-assisted transfer, where PMMA is often used as a carrier. Even after "cleaning", PMMA residues in the form of nanoparticles of about 100 nm in size remain on the surface of the monolayer MoS_2 [25]. These residues critically complicate the clean recovery of MoS_2 for reuse, as polymer contamination reduces the functional value of the recovered 2D material. For documenting and improving the overall environmental profile of a optico-electronic devices it needs to carry out a Life Cycle Assessment (LCA), in accordance with ISO 14040 and ISO 14044 [26]. Such performing an LCA will allow us to compare the carbon footprint of this bio-OLED with that of traditional OLEDs, which is critical for strategic positioning in the market, especially given that bioplastics are typically more expensive than conventional plastics. It is necessary to do because of Design for Disassembly (DfD) is a fundamental principle that involves designing new devices so that they can be easily disassembled for material recovery, reuse, or recycling [27]. The most critical challenge to the circular economy arises at the micro level — interlayer interfaces, especially between the PMMA polymer and the 2D material MoS_2. Therefore, DfD strategies should focus on creating selective dissociation mechanisms. The ideal solution is to introduce an intermediate, temporary or thermolabile interface layer that can be dissolved by an environmentally safe, moderately polar solvent (e.g., water or alcohol) or degraded by mild heating, allowing clean separation of the PMMA/Dye layer from MoS_2 without damaging it. An effective circular pathway for this hybrid system requires the development of an integrated three-step system that takes into account the unique chemical properties of each material. PMMA is one of the most suitable polymers for chemical recycling because it can be efficiently depolymerized back into the monomer MMA, which can then be reused in primary production.

To ensure the high purity of the monomer required for optical devices, it is critical to avoid contamination with organic dyes. After mechanical dismantling of the PMMA/Dye layer, a pre-treatment is required. This may involve mild solvolysis or oxidative degradation of the dispersed natural dyes to minimize their amount before pyrolysis. This step should be optimized to ensure biodegradation of the dyes. The procedure of thermal depolymerisation of the pre-purified PMMA promotes to obtain optical grade MMA monomer. This will allow the use of the recovered monomer to create new high-tech components. It is worth to note that natural dyes (chlorophylls) are bio-based components with circularity achieving not through chemical recycling, but, importantly, through returning to the biological cycle. A DfD process will need for effectively separating natural dyes for biodegradation, ensuring the purity of PMMA before its chemical recycling. To do this, PMMA-free MoS_2 transfer technologies need to be developed and validated.

4. Conclusions

In this study have demonstrated that the natural dyes with high-intensity PL can be used as color conversion layers, applied in organic light–emitting devices to achieve high performance. It was proposed construct the OLEDs using two natural dyes derivatives from noble fir leaves (*evergreen*) and blue hydrangea flowers, as the active PL dyes and underlined the impact of the dye optical properties on the emission performance. It was shown that the polymer composites based on natural dye-PMMA with high-purity fluorescence can be used as color conversion layers, applied in organic light–emitting devices. The optical properties of noble fir dye-PMMA and blue hydrangea dye-PMMA nanostructures were evaluated from measurements of the diffuse reflectance, ellipsometric characteristics and FTIR spectroscopy. Importantly, adding of ultrathin MoS_2 monolayer can

 doi:10.20944/preprints202511.2081.v1

significantly enhance the resulting intensity of the PL emitted by natural dye-PMMA nanostructures due to the overlapping of the spectra of PL emission from constitute layers and a strong back reflectance from MoS_2 nanostructure. It was shown that noble fir dye-PMMA and blue hydrangea dye-PMMA nanostructures can emit the light in red and green spectral region with a small FWHM. Such color purity is essential key criterion of OLEDs for future commercial displays.

Data Availability Statement: The data that support the findings of this study are available from the corresponding author upon reasonable request.

Acknowledgments: The work was performed with the support of Graphene Flagship programme, Core 3 (881603) and programme: "Improving the efficiency of decarbonization and greening of municipal energy by the method of optimized implementation of energy-saving technologies" of the National Academy of Sciences and Education of Ukraine (RN 0124U001473).

Conflicts of Interest: The authors declare no competing financial interests and no conflict of interest.

References

1. Zhang, J.; Zhao, S.; Jiang, J.; Lv, Z.; Luo, J.; Shi, Y.; Lu, Z.; Wang, X. Organic Cocrystal Alloys: From Three Primary Colors to Continuously Tunable Emission and Applications on Optical Waveguides and Displays. *Small* **2024**, *20*, e2400313, https://doi.org/10.1002/smll.202400313.
2. Liu, W.; Li, S.; Xie, Z.; Huang, K.; Yan, K.; Zhao, Y.; Redshaw, C.; Feng, X.; Tang, B.Z. Molecular Engineering toward Broad Color-Tunable Emission of Pyrene-Based Aggregation-Induced Emission Luminogens. *Adv. Opt. Mater.* **2024**, *12*, 2400301, https://doi.org/10.1002/adom.202400301.
3. Okoročenkova, J.; Filgas, J.; Khan, N.M.; Slavíček, P.; Klán, P. Thermal Truncation of Heptamethine Cyanine Dyes. *J. Am. Chem. Soc.* **2024**, *146*, 19768–19781, https://doi.org/10.1021/jacs.4c02116.
4. Song, J.; Lee, H.; Jeong, E.G.; Choi, K.C.; Yoo, S. Organic Light-Emitting Diodes: Pushing Toward the Limits and Beyond. *Adv. Mater.* **2020**, *32*, e1907539, https://doi.org/10.1002/adma.201907539.
5. Richhariya, G.; Kumar, A.; Tekasakul, P.; Gupta, B. Natural dyes for dye sensitized solar cell: A review. *Renew. Sustain. Energy Rev.* **2017**, *69*, 705–718, https://doi.org/10.1016/j.rser.2016.11.198.
6. Mondal, H.; Ray, S.K.; Chakrabarty, P.; Pal, S.; Gangopadhyay, G.; Das, S.; Das, S.; Basori, R. High-Performance Chlorophyll-b/Si Nanowire Heterostructure for Self-Biasing Bioinorganic Hybrid Photodetectors. *ACS Appl. Nano Mater.* **2021**, *4*, 5726–5736, https://doi.org/10.1021/acsanm.1c00517.
7. Swapna, M.S.; Raj, V.; Devi, H.V.S.; Sankararaman, S. Optical emission diagnosis of carbon nanoparticle-incorporated chlorophyll for sensing applications. *Photochem. Photobiol. Sci.* **2019**, *18*, 1382–1388, https://doi.org/10.1039/c8pp00454d.
8. Lee, C.-P.; Lin, R.Y.-Y.; Lin, L.-Y.; Li, C.-T.; Chu, T.-C.; Sun, S.-S.; Lin, J.T.; Ho, K.-C. Recent progress in organic sensitizers for dye-sensitized solar cells. *RSC Adv.* **2015**, *5*, 23810–23825, https://doi.org/10.1039/c4ra16493h.
9. Schiller, H.; Dau, H. Preparation protocols for high-activity Photosystem II membrane particles of green algae and higher plants, pH dependence of oxygen evolution and comparison of the S2-state multiline signal by X-band EPR spectroscopy. *J. Photochem. Photobiol. B: Biol.* **2000**, *55*, 138–144, https://doi.org/10.1016/s1011-1344(00)00036-1.
10. Kravets, V.G. Photoluminescence and Raman spectra of SnOx nanostructures doped with Sm ions. *Opt. Spectrosc.* **2007**, *103*, 766–771, https://doi.org/10.1134/s0030400x07110148.
11. Kravets, V.G. Using electron trapping materials for optical memory. *Opt. Mater.* **2001**, *16*, 369–375, https://doi.org/10.1016/s0925-3467(00)00096-3.
12. Meier, C.; Lüttjohann, S.; Kravets, V.G.; Nienhaus, H.; Lorke, A.; Ifeacho, P.; Wiggers, H.; Schulz, C.; Kennedy, M.K.; Kruis, F.E. Vibrational and defect states in SnOx nanoparticles. *J. Appl. Phys.* **2006**, *99*, 113108, https://doi.org/10.1063/1.2203408.
13. Kubelka, P. New Contributions to the Optics of Intensely Light-Scattering Materials Part II: Nonhomogeneous Layers*. *J. Opt. Soc. Am.* **1954**, *44*, 330–335, https://doi.org/10.1364/josa.44.000330.
14. Azzam, R.M.A.; Bashara, N.M. Ellipsometry and polarized light, North-Holland, Amsterdam, 1987.

 doi:10.20944/preprints202511.2081.v1

15. Kravets, V.G.; Grigorenko, A.N. Water and seawater splitting with MgB2 plasmonic metal-based photocatalyst. *Sci. Rep.* **2025**, *15*, 1–14, https://doi.org/10.1038/s41598-024-82494-5.
16. Kravets, V.G.; Wu, F.; Yu, T.; Grigorenko, A.N. Metal-Dielectric-Graphene Hybrid Heterostructures with Enhanced Surface Plasmon Resonance Sensitivity Based on Amplitude and Phase Measurements. *Plasmonics* **2022**, *17*, 973–987, https://doi.org/10.1007/s11468-022-01594-y.
17. Born, M.; Wolf, E.; Bhatia, A.B.; Clemmow, P.C.; Gabor, D.; Stokes, A.R.; Taylor, A.M.; Wayman, P.A.; Wilcock, W.L. *Principles of Optics*; Cambridge University Press (CUP): Cambridge, United Kingdom, 1999; ISBN: .
18. Kravets, V.G.; Zhukov, A.A.; Holwill, M.; Novoselov, K.S.; Grigorenko, A.N. "Dead" Exciton Layer and Exciton Anisotropy of Bulk MoS_2 Extracted from Optical Measurements. *ACS Nano* **2022**, *16*, 18637–18647, https://doi.org/10.1021/acsnano.2c07169.
19. Kravets, V. Ellipsometry and optical spectroscopy of low-dimensional family TMDs. *Semicond. Physics, Quantum Electron. Optoelectron.* **2017**, *20*, 284–296, https://doi.org/10.15407/spqeo20.03.284.
20. Brouwer, A.M. Standards for photoluminescence quantum yield measurements in solution (IUPAC Technical Report). *Pure Appl. Chem.* **2011**, *83*, 2213–2228, https://doi.org/10.1351/pac-rep-10-09-31.
21. *Photobiology*; Springer Nature: Durham, NC, United States, 2015; ISBN: .
22. Larkum, A.W.; Kühl, M. Chlorophyll d: the puzzle resolved. *Trends Plant Sci.* **2005**, *10*, 355–357, https://doi.org/10.1016/j.tplants.2005.06.005.
23. Hussain, M.; Jalali, T.; Maftoon-Azad, L.; Osfouri, S. Performance Evaluation of Natural Dye-Sensitized Solar Cells: A Comparison of Density Functional Theory and Experimental Data on Chlorophyll, Anthocyanin, and Cocktail Dyes as Sensitizers. *ACS Appl. Electron. Mater.* **2024**, *6*, 1693–1709, https://doi.org/10.1021/acsaelm.3c01618.
24. Fennel, F.; Lochbrunner, S. Long distance energy transfer in a polymer matrix doped with a perylene dye. *Phys. Chem. Chem. Phys.* **2011**, *13*, 3527–3533, https://doi.org/10.1039/c0cp01211d.
25. Bhuyan, C.A.; Madapu, K.K.; Prabakar, K.; Das, A.; Polaki, S.R.; Sinha, S.K.; Dhara, S. A Novel Methodology of Using Nonsolvent in Achieving Ultraclean Transferred Monolayer MoS_2. *Adv. Mater. Interfaces* **2022**, *9*, 2200030. https://doi.org/10.1002/admi.202200030.
26. Finkbeiner, M. The International Standards as the Constitution of Life Cycle Assessment: The ISO 14040 Series and its Offspring, in: W. Klöpffer (Ed.), Background and Future Prospects in Life Cycle Assessment, Springer Netherlands, Dordrecht, 2014: pp. 85–106. https://doi.org/10.1007/978-94-017-8697-3_3.
27. Tsoka, S.; Tsikaloudaki, K. Design for Circularity, Design for Adaptability, Design for Disassembly, in: Bragança, L.; Griffiths, P.; Askar, R.; Salles, A.; Ungureanu, V.; Tsikaloudaki, K.; Bajare, D.; Zsembinszki, G.; Cvetkovska, M. (Eds.), Circular Economy Design and Management in the Built Environment, Springer Nature Switzerland, Cham, 2025: pp. 257–272. https://doi.org/10.1007/978-3-031-73490-8_9.